"unhappy force fit" and rather severe "rounding" of the transition. This type of divergence is the sort predicted by the classical Ornstein-Zernike approximation[20] and also the type of divergence predicted *above* T_c by the exact solution to the two-dimensional analog of the KDP problem.[21] In Fig. 5(b) we plot C_G versus $\log_{10}(T_c-T)$ and attempt to fit the data to a logarithmic divergence. If anything, as in the case of KDP, the logarithmic divergence appears to be a slightly better fit than the power-law divergence, although the lack of sufficient data in the range $T_c-T<0.1°$ makes the analysis questionable. The preference for the logarithmic fit is perhaps made a bit stronger when we recall that the region of this fit, $T>219°$K, is precisely the region in which the data deviate strongly from the mean-field theory.

In conclusion, then, we find the transition to be of first order. We find that the SUS theory can give a reasonable account of the thermodynamic properties of DKDP in the region more than about 1°K away from T_c if we use the parameters $\epsilon_0/k=94.3°$K, $\epsilon_1/k=900°$K, and $\beta/k=35.6°$K. While an apparently reasonable set of parameters for describing the disordering contribution of the heat capacity of KDP can be obtained by scaling these parameters for the purpose of deducing the lattice-heat capacity, it is pointed out that these scaled parameters lead to contradictions with experiment in the case of KDP, so that more elaborate theories of the tunneling type are probably needed for a complete description of KDP. Finally, it is pointed out that the critical region in DKDP probably lies between 219°K and T_c and the divergence of the heat capacity is best described by a logarithmic divergence in this region.

[20] R. Brout, *Phase Transitions* (W. A. Benjamin, Inc., New York, 1964).

[21] E. H. Lieb, Phys. Rev. Letters **18**, 692 (1967); **18**, 1046 (1967); **19**, 108 (1967); B. Sutherland, *ibid.* **19**, 103 (1967); C. P. Yang, *ibid.* **19**, 586 (1967); B. Sutherland, C. N. Yang, and C. P. Yang, *ibid.* **19**, 588 (1967).

PHYSICAL REVIEW VOLUME 167, NUMBER 2 10 MARCH 1968

Crystal Dynamics and Magnetic Excitations in Cobaltous Oxide

J. SAKURAI,* W. J. L. BUYERS, R. A. COWLEY, AND G. DOLLING

Chalk River Nuclear Laboratories, Chalk River, Ontario, Canada

(Received 21 August 1967)

The low-lying phonon and magnetic excitations of CoO have been studied experimentally and theoretically, both above and below the antiferromagnetic ordering temperature. The experiments were performed using the technique of inelastic scattering of slow neutrons with the aid of a triple-axis crystal spectrometer. These experiments were difficult because the phonon and magnetic excitations have very similar frequencies, and also because the specimen has a domain structure in the antiferromagnetic phase. Nevertheless, models were obtained for the phonon spectra. The magnetic spectra of the paramagnetic phase can be understood if the spin-orbit coupling parameter of Co^{2+} of CoO is reduced to 40% of its free-ion value. With this value it is then possible to understand the excitations in the antiferromagnetic phase in at least a qualitative way by introducing nearest- and next-nearest-neighbor exchange parameters. A detailed evaluation of this theory of the magnetic excitations is not possible, because of the difficulties encountered in the experimental part of the study; nevertheless, it is believed that the description given here is essentially correct.

I. INTRODUCTION

THE magnetic properties of cobaltous oxide (CoO) are of considerable interest both theoretically and experimentally. Experimentally it is of interest that CoO is an antiferromagnet with a high Néel temperature, about 293°K, and in its paramagnetic phase it has the cubic NaCl structure. From the theoretical aspect CoO is of interest because the Co^{2+} ion has orbital angular momentum which is not quenched entirely by the cubic crystalline field. There are some low-lying excited states of the Co^{2+} ion, and it is of interest to determine the extent to which they modify the magnetic properties.

In its antiferromagnetic phase, CoO has a tetragonal crystal structure in which the atomic magnetic moments are arranged in ferromagnetic sheets in (111) crystallographic planes.[1–3] There is some doubt[3] concerning the actual alignment of the moments in each plane, because the data obtained from neutron-diffraction experiments on single-crystal specimens may be interpreted in terms of either the collinear spin model of Roth[1] or by the multispin axis model of van Laar.[2] At present, the weight of evidence favors the collinear spin model, particularly in view of the recent experiments by Saito *et al.*[4] Measurements have been made of the

* Visiting Fellow; present address: Physics Department, Iowa State University, Ames, Iowa.

[1] W. L. Roth, Phys. Rev. **110**, 1333 (1958).

[2] B. van Laar, Phys. Rev. **138**, A584 (1965).

[3] B. van Laar, J. Schweizer and R. Lemaire, Phys. Rev. **141**, 538 (1966).

[4] S. Saito, K. Nakahigashi, and Y. Shimomura, J. Phys. Soc. Japan **21**, 580 (1966).

magnetic susceptibility[5] and anisotropy[6] of CoO, and also of its infrared absorption spectrum.[7–9]

Several studies have been made of the energy levels of Co^{2+}, and in particular a detailed discussion of the properties of CoO, including the effects of the lower excited electronic states of the Co^{2+} ions, has been given by Kanamori[10] and Tachiki.[11] Experimentally, difficulties may arise in the interpretation of experiments on single-crystal specimens if the specimen does not consist of a single domain. On cooling through the Néel temperature ($T_N = 293°K$), the tetragonal distortion occurs along any of the three original cube axes, so that, with the four possible choices of orientation of the ferromagnetic sheets within each tetragonal domain, there are a total of 12 different domains. Although the production of essentially single-domain crystals by careful control of the temperature gradient direction during cooling seems to be a practical possibility,[6] this was not attempted in the present experiments. The primary object of these experiments was to determine the dispersion relation between the energy (or frequency) and wave vector of the magnetic excitations in CoO by inelastic scattering of slow neutrons. The normal modes of vibration of the material were also studied, both above and below T_N, and a search for evidence of magnon-phonon interaction was also carried out.

The determination of magnon and phonon dispersion relations may be performed by observing the coherent, inelastic scattering of slow neutrons by single-crystal specimens.[12] A monoenergetic beam of neutrons (energy E_0, momentum $\hbar\mathbf{k}_0$) is incident upon the specimen, and scattering processes may occur in which one quantum of the excitations (magnons, phonons, etc.) is created or annihilated. The scattered neutrons now have energy E' and momentum $\hbar\mathbf{k}'$, and application of the laws of conservation of energy and "crystal momentum" permit the determination of the energy $h\nu$ and reduced wave vector $\mathbf{q}$ of the excitation involved:

$$E_0 - E' = \pm h\nu, \tag{1}$$

$$\mathbf{k}_0 - \mathbf{k}' = \mathbf{Q} = 2\pi\boldsymbol{\tau} + \mathbf{q}. \tag{2}$$

$\mathbf{Q}$ is the momentum transfer vector and $\boldsymbol{\tau}$ is a vector of the reciprocal lattice of the crystal. The observation of these "one-phonon" or "one-magnon" processes may be conveniently made by means of a triple-axis crystal spectrometer.[13] A brief description of the experiments is given in Sec. II, together with the results obtained at temperatures both above and below T_N. Some of the excitations observed may be identified as phonons and these will be discussed and analyzed in Sec. III. In addition to these excitations two further branches were observed which are believed to arise from the magnetic excitations. These are discussed in Sec. IV, where it is shown that they may be explained quite readily, if somewhat surprisingly, if the spin-orbit coupling parameter in the crystal is only 40% that of the free ion. The results are summarized in a concluding section.

II. EXPERIMENTS AND RESULTS

The specimen of CoO employed in these experiments consisted of four irregular single-crystal boules mounted in a vertical plane with their axes roughly parallel. Each crystal could be tilted and rotated independently to produce a crystallographic orientation common to all, viz., a (110) axis normal to the horizontal plane containing the incident and scattered neutron beams. The effective mosaic spread of this composite specimen was 0.35 deg. Experiments at 110, 330 and 425°K were carried out with the specimen inside a liquid-nitrogen cryostat fitted with suitable heating coils and radiation shields.

All of the experiments were performed with the triple-axis crystal spectrometer at the C5 facility of the NRU reactor, Chalk River. The spectrometer was operated throughout in a "constant-Q" mode,[13] in which the incident neutron energy, angle of scattering, and sample orientation are varied simultaneously (keeping the scattered neutron energy constant) in such a way that the momentum-transfer vector $\mathbf{Q}$ [Eq. (2)] remains constant. In this way one obtains the scattered neutron energy distribution for a preselected value of the reduced wave vector $\mathbf{q}$. The present measurements were confined to wave vectors $\mathbf{q}$ along three directions of high symmetry, (00ζ), $(\zeta\zeta 0)$, and $(\zeta\zeta\zeta)$, where $2\pi\zeta/a$ is a coordinate of $\mathbf{q}$ (a is the lattice constant). Throughout this paper we shall for convenience refer to symmetry axes and wave vectors appropriate to the high-temperature cubic phase of CoO, even when we are dealing with the low-temperature tetragonal phase. Owing to the small size of the tetragonal distortion, and the multidomain character of our specimen, we are unable to distinguish between excitations propagating along the a or c axes.

Some typical scattered neutron distributions are shown in Figs. 1, 2, and 3. In Fig. 1 the results of scans with a wave-vector transfer $\mathbf{Q}$ of $(2, 2, 0)2\pi/a$ at 425 and 110°K are shown. The peaks are not believed to arise from scattering by the phonons, but from magnetic excitations. The results clearly show the presence of

[5] C. H. La Blanchetais, J. Phys. Radium **12**, 765 (1951).
[6] E. Uchida, N. Fukuoka, H. Kondoh, T. Takeda, Y. Nakazumi, and T. Nagamiya, J. Phys. Soc. Japan **19**, 2088 (1964).
[7] R. Newman and R. M. Chrenko, Phys. Rev. **115**, 1147 (1959).
[8] P. J. Gielisse, L. C. Mansur, R. Marshall, S. S. Mitra, R. Mykolajewycz, J. N. Plendl, and A. Smakula, J. Appl. Phys. **36**, 2446 (1965).
[9] R. C. Milward, Phys. Letters **16**, 244 (1965).
[10] J. Kanamori, Progr. Theoret. Phys. (Kyoto) **17**, 177 (1956); **17**, 197 (1956).
[11] M. Tachiki, J. Phys. Soc. Japan **19**, 454 (1964).
[12] See *Thermal Neutron Scattering*, edited by P. A. Egelstaff (Academic Press Inc., New York, 1965), Chaps. 1, 5, and 6.
[13] B. N. Brockhouse, in *Inelastic Scattering of Neutrons in Solids and Liquids* (International Atomic Energy Agency, Vienna, 1961) p. 113.

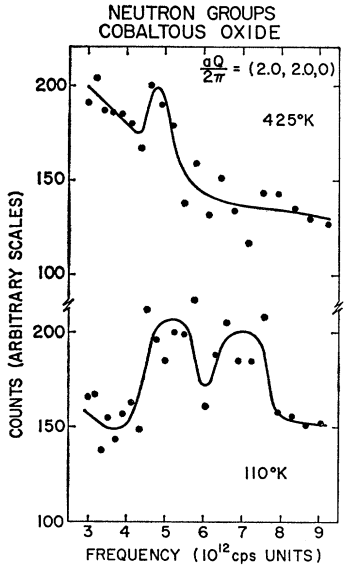

FIG. 1. Observed neutron groups for two "constant-Q" scans at 110 and 425°K. The peaks are believed to arise largely from magnetic scattering, and show the decrease in intensity at a frequency of 7.0 at 425°K. The rise in intensity at low frequency at 425°K is associated with the paramagnetic scattering.

some scattering with a frequency of about 5×10^{12} cps at both temperatures, and further scattering with a frequency of 7×10^{12} at 110°K. Figure 2 shows two distributions obtained at 110°K, for wave vectors close to the (002) reciprocal-lattice point. The peaks marked M1 and M2 are believed not to arise from coherent one-phonon scattering processes. The peak marked LA, however, arises from scattering by the longitudinal acoustic phonon propagating along the (00ζ) direction.

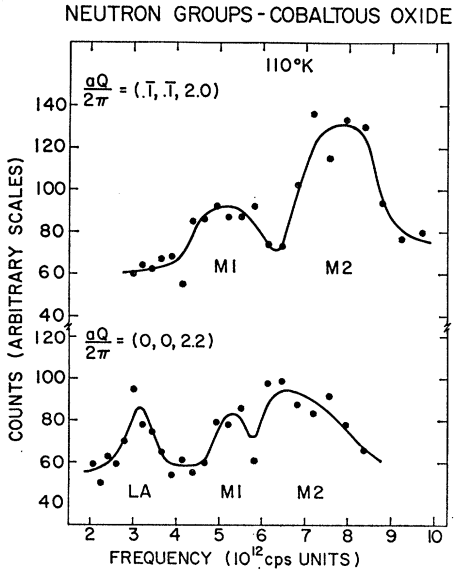

FIG. 2. Two distributions obtained at 110°K. The peaks labeled M1 and M2 are from the magnetic excitations and LA from the longitudinal acoustic normal mode of vibration.

In Fig. 3 is shown a distribution obtained near the reciprocal-lattice point (004), and shows the presence of the 'magnetic' excitations at 425°K. The complete results at 110°K are shown in Fig. 4. The initial results in the paramagnetic phase were obtained for $\mathbf{q}$ along the cube body diagonal (Λ), at a temperature of 330°K. Subsequent measurements for the other two high-symmetry directions (Δ, Σ) were made at 425°K, and Fig. 5 is a composite of all these high-temperature results.

Standard group-theoretical methods were used in conjunction with the character tables of Koster,[14] to label the various branches of these spectra that could be identified with phonon excitations. [The labeling of branches at the point X (or M) was given incorrectly by Cochran *et al.*[15]] Considerable experimental difficulty was experienced, however, in making assignments within the frequency range 4.5 to 7.5×10^{12} cps, owing to the presence of two broad bands of frequencies which

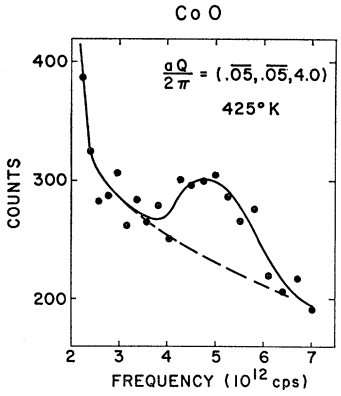

FIG. 3. A distribution at 425°K showing a magnetic excitation.

were approximately independent of wave vector, and which are believed to arise from scattering by the magnetic excitations. We shall label the lower and upper broad bands M1 and M2, respectively. At 110°K, both bands gave rise to neutron scattering of comparable intensity, but at 425°K the intensity from the upper band was only just observable. The lower-frequency band was still readily observed, however. The variation in the intensity of these bands as a function of momentum transfer was difficult to determine because of the presence of phonons with similar frequencies. However, where phonon scattering is likely to be unimportant, the intensity decreased somewhat as the momentum transfer increased.

III. PHONON EXCITATIONS

The neutron groups corresponding to scattering from transverse acoustic and optic modes of vibration could

[14] G. C. Koster, in *Solid State Physics*, edited by F. Seitz and D. Turnbull (Academic Press Inc., New York, 1957), Vol. 5, p. 174.

[15] W. Cochran, R. A. Cowley, G. Dolling, and M. M. Elcombe, Proc. Roy. Soc. (London) **A293**, 433 (1966).

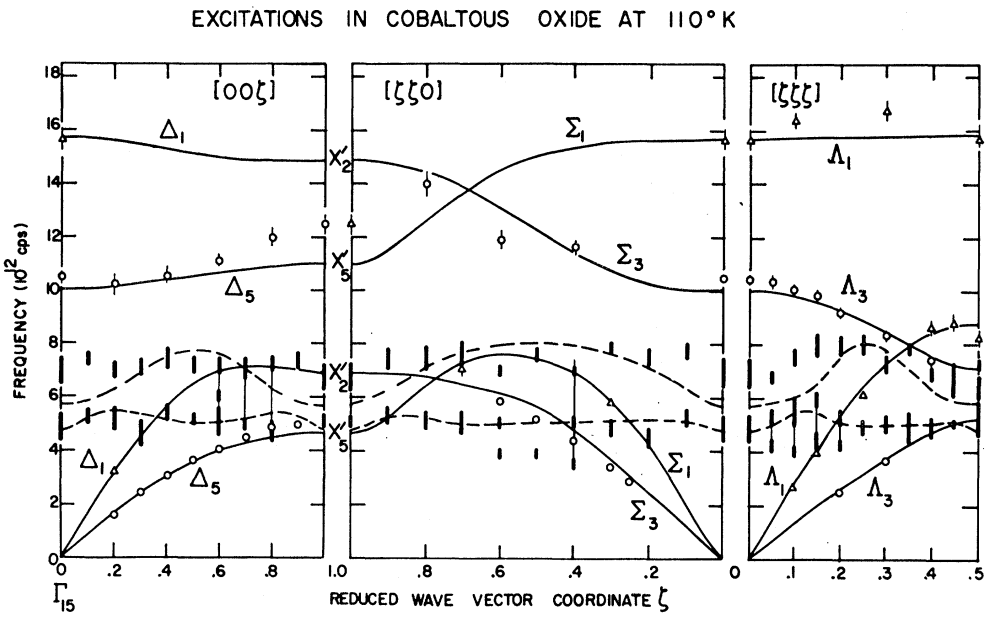

FIG. 4. The complete experimental results at 110°K. The circles (transverse modes) and triangles (longitudinal modes) arise from sharp peaks in the scattered distributions, while the bars represent the broad peaks. The thin lines connecting the bars indicate the presence of weaker intensity near the broad peaks. The labels are the standard group theoretical labels (See Ref. 14) for the phonon branches in the NaCl structure. The solid lines show a best-fit shell model to the phonon-dispersion curves, and the dotted lines a magnon model with second nearest-neighbor interaction.

in many cases be identified unambiguously. The frequency of the transverse optic mode with small q is in good agreement with the infrared-absorption results of Gielisse *et al.*[8] The assignment of longitudinal acoustic (LA) modes was more difficult, and two distinct interpretations of the low-temperature data of Fig. 4 seemed equally plausible at first sight. One might assume either (a) that the LA branches, after the initial steep slope at small q, leveled off rather abruptly near the M1 band to a constant frequency of 5×10^{12} cps, or (b) that they continued their initial slope to higher frequencies, in the vicinity of the upper band (M2) of excitations at 7 to 8×10^{12} cps. Though it was not possible definitely to resolve this ambiguity experimentally at 110°K, the indications were that alternative (b) was more likely, and these indications were stronger at higher temperatures. This also appears more likely on comparing these dispersion curves with those of alkali halides.[16]

A consistent set of measured phonon frequencies was arrived at for both alternatives (a) and (b), and in each case, attempts were made to fit the 425°K measurements on the basis of the dipole-approximation model.[15,16] This model has been fully described elsewhere; details of the notation used in this paper are given in Ref. 15. Three versions of the model were used in the present least-squares fitting process: (i) the "simple shell model,"[16] in which the ionic charge is fixed at 2.00, central short-range repulsive forces are postulated between nearest-neighbor ions, and only the oxygen ion is assumed to be polarizable; (ii) a rigid-ion model,[17] in which the ionic charge is allowed to vary, axially symmetric forces are postulated between first and second nearest-neighbor ions, and neither ion is polarizable; (iii) a more general model obtained from model (ii) by allowing both Co^{++} and O^{--} ions to be polarizable. These models have 3, 7, and 11 disposable parameters, respectively. Only model (iii) was found to be capable of providing a fit to the phonon frequencies that was comparable with the experimental accuracy, and a slightly better fit was obtained if the LA modes were interpreted according to scheme (b) above. The solid curves shown in Figs. 4 and 5 are the results obtained at the two temperatures on the basis of model (iii), with the LA modes assigned according to alternative (b). Except perhaps for the transverse optic modes (Δ_5) near the zone boundary point X, the fit to the data is quite satisfactory.

Some of the results of the least-squares fitting procedure are given in Table I. Comparing the values of the parameters of model (iii) obtained at 425°K, we see that alternative (b) leads to a higher ionic charge than (a), higher nearest-neighbor force constants and lower second-nearest-neighbor constants. These are physically reasonable features of the model, and suggest that the LA modes do reach frequencies in the range 7 to 8×10^{12} cps at large wave vectors. These models and the fits obtained by this approach must be regarded as only tentative in view of the existence of the M1 and M2

[16] A. D. B. Woods, W. Cochran, and B. N. Brockhouse, Phys. Rev. **119**, 980 (1960).

[17] E. W. Kellerman, Phil. Trans. **A238**, 513 (1940).

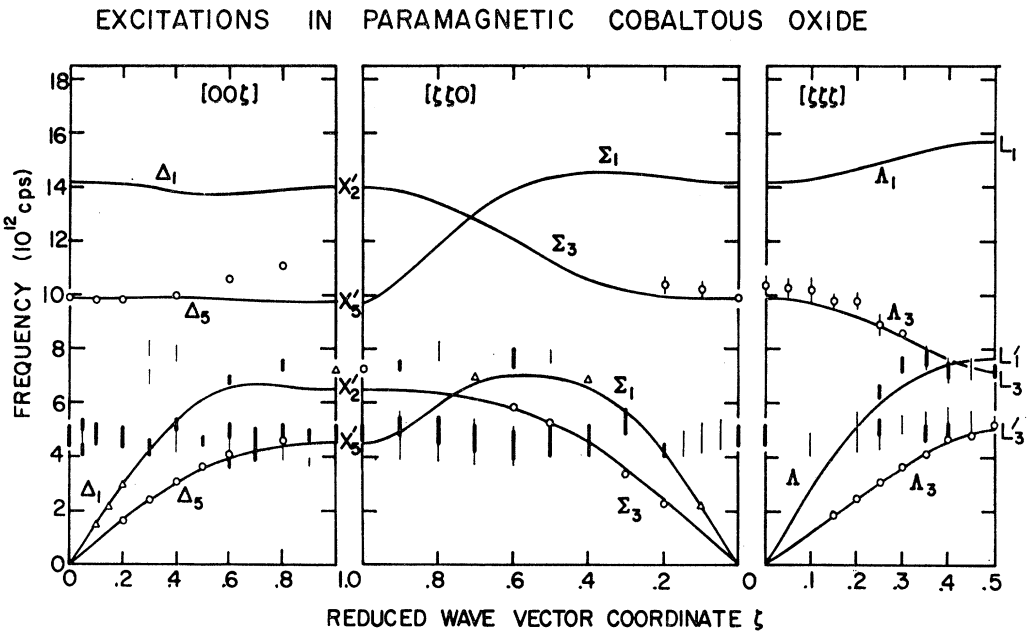

FIG. 5. The experimental results in the paramagnetic phase of CoO. The results for the [00ζ] and [ζζ0] directions are at 425°K and [ζζζ] at 330°K. The circles (transverse modes) and triangles (longitudinal modes) arise from sharp peaks, and the bars from broad peaks. The thin vertical bars indicate broad distributions of low intensity. The solid lines are a shell-model best fit to the phonon-dispersion curves. The magnetic curves are then seen to be a flat branch at a frequency of 4.8 and a weaker branch at about 7.8.

excitations in the same frequency range, which almost certainly would influence the phonon-dispersion curves. Intermixing of phonon modes with other excitations such as plasmons and magnons has been previously observed in neutron inelastic-scattering experiments.[18,19] This matter will be discussed in the next section.

From the slopes of the acoustic-phonon modes for small values of q in the three high-symmetry directions in CoO, we may obtain estimates of the elastic constants appropriate for "zero-sound" propagation.[20] The values of the elastic constants can best be estimated by use of the harmonic models of Table I. Although these elastic constants are strictly not the same as those deduced from ultrasonic measurements, which have not yet been made for CoO, the differences are certainly less than the error on the model elastic constants (5–10%). Table II lists these elastic constants and also the high- and low-frequency dielectric constants derived from model (iii) (b) at both 425 and 110°K. It may be seen that the model predicts dielectric constants in reasonable agreement with their observed values.

IV. MAGNETIC EXCITATIONS

1. General Description

From a consideration of Figs. 4 and 5 and of the force model calculations of the previous section, it is evident that there exist in CoO, both at 425 and 110°K, certain bands of excitations which cannot be accommodated within the framework of the lattice dynamics of a cubic diatomic crystal. In this section we discuss to what extent these bands may be associated with the magnetic properties of cobaltous oxide.

Kanamori[10] has given a detailed description of the behavior of the Co^{2+} ion in CoO and his treatment has been extended by Tachiki[11] to calculate the anti-

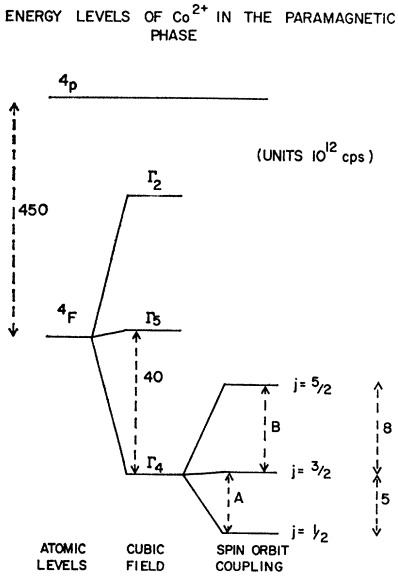

FIG. 6. The energy-level diagrams of $Co^{+\,+}$, in the paramagnetic state, showing the effects of the cubic crystal field, and the spin-orbit interaction.

[18] R. A. Cowley and G. Dolling, Phys. Rev. Letters **14**, 549 (1965).
[19] G. Dolling and R. A. Cowley, Phys. Rev. Letters **16**, 683 (1966).
[20] R. A. Cowley, Proc. Phys. Soc. (London) **90**, 1127 (1967).

TABLE I. Best-fit values of the parameters[a] of some interatomic-force models for CoO. The short-range force constants (A to B'') are quoted in units of ($e^2/2v$), where v is the volume of the primitive unit cell. The assignment of the LA mode frequencies according to scheme (a) or (b) is discussed in the text. χ is a measure of the quality of the fit to the data in each case.

Model	(*i*)	(*i*)	(*i*)	(*ii*)	(*iii*)	(*iii*)	(*iii*)
Temperature (°K)	425	425	110	425	425	425	110
LA modes	(a)	(b)	(b)	(b)	(a)	(b)	(b)
Co–O							
A	28.51	29.40	31.13	8.96	14.65	21.98	35.93
B	−4.66[b]	−4.66[b]	−4.66[b]	0.21	−0.31	−2.35	−5.54
Co–Co							
A'	···	···	···	1.25	−2.19	−0.21	−3.80
B'	···	···	···	−0.07	0.58	0.04	0.68
O–O							
A''	···	···	···	4.20	6.95	1.94	1.18
B''	···	···	···	−1.21	−2.25	−1.11	−1.22
Z (e)	2.0[b]	2.0[b]	2.0[b]	0.82	1.20	1.58	2.06
α_1 (10^{-24} cm^3)	···	···	···	···	0.085	0.082	0.071
d_1 (e)	···	···	···	···	−0.19	−0.50	−0.58
α_2 (10^{-24} cm^3)	0.143	0.144	0.142	···	0.065	0.083	0.105
d_2 (e)	1.49	1.02	1.03	···	0.43	0.51	0.95
χ	7.93	7.30	5.75	6.13	2.47	2.13	2.30

[a] The detailed definitions of the parameters are given in Ref. 15.
[b] The ionic charge is kept fixed and the force constant B determined from the equilibrium condition as described in Ref. 16.

ferromagnetic resonance frequencies. The single-ion energy-level diagram of Co^{2+} in CoO is shown in Fig. 6. The ground-state ^4F configuration of the free ion is split by the cubic field to give a Γ_4 orbital triplet of lowest energy. The spin-orbit coupling then further reduces the degeneracy of this effective $l=1$ state to give three states described by quantum numbers $j=\frac{5}{2}, \frac{3}{2}, \frac{1}{2}$. The lowest of these is a Kramers doublet with $j=\frac{1}{2}$. Kanamori estimates the energy of the $j=\frac{3}{2}$ and $j=\frac{5}{2}$ states above this $j=\frac{1}{2}$ state to be 12.1 and 32.4×10^{12} cps, respectively, by using the free-ion spin-orbit coupling parameter λ.

2. Interpretation of Paramagnetic Excitations

In the paramagnetic phase the experimental results show a strong band (M1) of frequency about 4.8 and a much weaker band (M2) at 7.8. Since both of these bands are very flat they arise almost entirely from the properties of single ions and it is tempting to identify them with the transitions A, Fig. 6, between the $j=\frac{1}{2}$ and $j=\frac{3}{2}$ levels, and, B, between the $j=\frac{3}{2}$ and $j=\frac{5}{2}$ levels. The latter transition is weaker both because there are fewer ions in the $j=\frac{3}{2}$ state than in the $j=\frac{1}{2}$ state at 425°K, and also because its higher frequency leads to a smaller neutron cross section. The even weaker intensity of the M2 band observed at 330°K, is consistent with this interpretation. This identification of the M1 and M2 bands in the paramagnetic phase is supported by the observed ratio of their frequencies. If the bands are due to spin-orbit levels, then their ratio should be a constant, 0.60, independent of the coupling parameter. Experimentally, this ratio is found to be 0.61 ± 0.07, in excellent agreement with theory for spin-orbit splitting. However, in order to give the observed energies, this scheme requires a reduction in the spin-orbit coupling parameter λ of the ion from -5.4×10^{12} cps in the free state, to -2.13×10^{12} cps in the crystal.

TABLE II. Values of elastic and dielectric constants derived from the harmonic force models (iii) (b) of Table I.

Temperature (°K)	Derived from model 425	Derived from model 110	Experimental 296
C_{11} (10^{12} dyn/cm^2)	27.7	30.7	
C_{12} (10^{12} dyn/cm^2)	18.0	18.3	
C_{44} (10^{12} dyn/cm^2)	9.1	9.0	
ϵ_∞	5.19	5.28	5.3
ϵ_0	10.70	12.73	12.19

3. Interpretation of Antiferromagnetic Excitations

In the antiferromagnetic state the results show two almost constant-frequency branches, again suggesting that the results may be explained largely by the single ion properties. The effect of applying a molecular field to the unperturbed spin-orbit states of Co^{2+} is shown in Fig. 7. The degeneracy of all the j multiplets is removed to give a complicated energy-level spectrum.

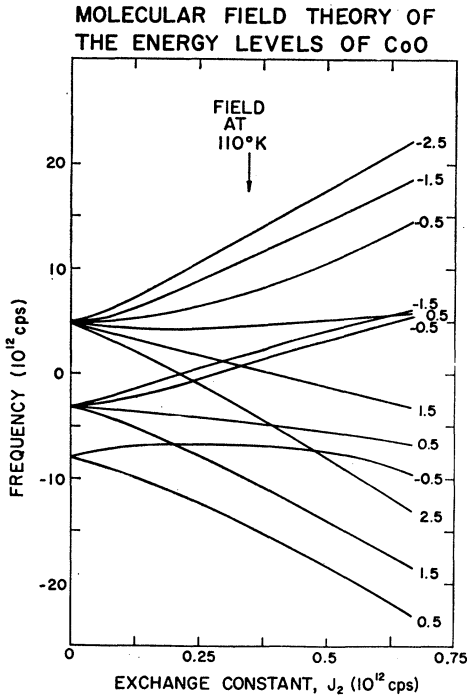

FIG. 7. The energy levels of the ground-state multiplet of Co^{2+} in the antiferromagnetic state, as a function of second-nearest-neighbor exchange parameter. The arrow shows the value of J_2 which gives the correct splitting for the lowest two states in CoO. The spin-orbit coupling parameter is $\lambda=-2.13\times10^{12}$ cps, and the tetragonal distortion is not included. The numbers at the right-hand side give the z component of the total angular momentum, $j=l+S$, of each state.

It is perhaps worth noting that the calculations were performed within the molecular-field approximation by introducing a Heisenberg exchange interaction J_2 between next-nearest neighbors. (Nearest neighbors do not contribute to the molecular field). The calculations were then performed self-consistently to obtain the energy levels shown in Fig. 7. The results show that an exchange interaction of $(0.347\pm0.02)\times10^{12}$ cps gives rise to two levels $(4.5$ and $7.8)\times10^{12}$ cps of close to the same frequency as those observed experimentally. However, the frequency of the first excited state is slightly lower than that observed (5.0). Good agreement for both states is obtained when we allow for a small tetragonal distortion of the crystal by adding a term cl_z^2 to the Hamiltonian, with c chosen to be -0.7 ± 0.2. The single-ion Hamiltonian is then of the form

$$\lambda'\mathbf{l}\cdot\mathbf{S}+cl_z^2+2J_2Z_2\langle S\rangle_{\rm av}S^z,$$

where $\lambda'=-\frac{3}{2}\lambda$ and Z_2 is the number of next-nearest neighbors. Kanamori's values[10] for these parameters are $J_2=0.45$ and $c=-3.0$.

4. Spin Waves in CoO

The introduction of a spin-wave model based on these crystal-field parameters will now be described. The Hamiltonian of the magnetic electrons in the Γ_4 state is taken to be

$$\sum_i[\lambda'\mathbf{l}(i)\cdot\mathbf{S}(i)+cl_z^2(i)]+\sum_{ij}J(ij)\mathbf{S}(i)\cdot\mathbf{S}(j),$$

The exchange interactions are taken to be of the Heisenberg form and restricted to nearest and second nearest neighbors. The spin waves for the magnetic excitations to the lowest two excited states of the Co^{2+} can be calculated for this model by use of the pseudo-boson techniques described, for example, by Grover.[21] Creation and destruction operators are introduced to describe excitations to the first $(a_1^\dagger, a_1)$ and second $(a_2^\dagger, a_2)$ excited state of a single ion. The spin operators at a particular site are then represented at low temperatures within this approximation by the relations

$$S^+=C_1a_1^\dagger+C_2a_2,\qquad S^-=C_1a_1+C_2a_2^\dagger,$$
$$S^z=C_3+C_4a_1^\dagger a_1+C_5(a_2^\dagger a_2),$$

where the coefficients are given by the matrix elements

$$C_1=\langle e_1\mid S^+\mid g\rangle,\qquad C_2=\langle e_2\mid S^-\mid g\rangle,$$
$$C_3=\langle g\mid S^z\mid g\rangle,\qquad C_4=\langle e_1\mid S^z\mid e_1\rangle-C_3,$$
$$C_5=\langle e_2\mid S^z\mid e_2\rangle-C_3.$$

The quadratic part of the Hamiltonian then becomes

$$\sum_i\Delta(1)a_1^\dagger(i)a_1(i)+\Delta(2)a_2^\dagger(i)a_2(i)$$
$$+\sum_{ij}^{L}J(ij)[C_1a_1^\dagger(i)+C_2a_2(i)][C_1a_1(j)+C_2a_2^\dagger(j)]$$
$$+\tfrac{1}{2}\sum_{ij}^{D}J(ij)[C_1a_1^\dagger(i)+C_2a_2(i)][C_1a_1^\dagger(j)+C_2a_2(j)]$$
$$+\text{c. c.},$$

where $\Delta(1)$ and $\Delta(2)$ are the single-ion frequencies within the molecular-field approximation, and $\sum^L$ and $\sum^D$ are summations over ions of the same and different spins, respectively. The frequencies of the spin waves can then be obtained from this Hamiltonian in the usual way.[22] The results using J_2 deduced from the molecular-field theory and with J_1 set to zero are shown by the dotted lines in Fig. 4. Clearly, they are in at least qualitative agreement with experiment. It is perhaps worth commenting that on this model the dispersion curves are identical for each domain.

The above model, which neglects nearest-neighbor interaction, is satisfactory as long as J_1 is small compared with J_2. J_1 may be deduced from paramagnetic-susceptibility measurements as described by Kanamori.[10]

The susceptibility depends only on the sum of the nearest and next-nearest exchange interaction $K=$

[21] B. Grover, Phys. Rev. **140**, A1944 (1965).
[22] L. R. Walker, in *Magnetism I*, edited by G. T. Rado and H. Suhl (Academic Press Inc., New York, 1965).

$2J_1Z_1+2J_2Z_2$, and on functions of the z components of angular-momentum operators. The thermal average over the unperturbed spin-orbit levels of such a function, for example, l^zS^z, will be written $\langle lS\rangle$, where

$$\langle lS\rangle=\sum_n\langle n\mid l^zS^z\mid n\rangle\exp(-\beta E_n)/\sum_n\exp(-\beta E_n).$$

The energy E_n is multiplied by $\beta=1/kT$. The paramagnetic susceptibility χ in the molecular-field approximation is then given by

$$\frac{\chi}{\mu_B{}^2\beta}=\frac{\langle(2S-\frac{3}{2}l)^2\rangle+\beta k(\frac{3}{2})^2(\langle l^2\rangle\langle S^2\rangle-\langle lS\rangle^2)}{1+\beta K\langle S^2\rangle}.$$

Although this expression does not have the form of the Curie-Weiss law, its denominator may be used to define a temperature

$$\Theta=K\langle S^2\rangle/k,$$

which we associate with the Curie temperature of -280°K, measured by La Blanchetais.[5] This leads to a value for K of 4.66×10^{12} cps and consequently a value for J_1 of 0.021×10^{12} cps. The paramagnetic susceptibility then agrees with the measurements of La Blanchetais[5] to within 15% over the range 400 to 900°K. An improved agreement should be possible if the higher excited states of the free ion are considered, as described by Kanamori.[10]

The dispersion curves for magnons below the transtion temperature were recalculated, including the nearest-neighbor exchange constant $J_1=0.021$. The frequencies differed by no more than 0.2×10^{12} cps from those obtained with $J_1=0$. Thus the agreement with experiment is not significantly improved by including the nearest-neighbor exchange constant. However, it does lead to different dispersion relations for the different domains, but in all cases the frequency difference is less than 0.2×10^{12} cps.

In practice the dispersion relations are even more complex because the spin direction is not along the tetragonal axis but tilted through 10°. This arises largely because of the magnetic dipolar anisotropy associated with the (111) ordering planes, and this anisotropy will split the doubly degenerate spin-wave modes for each domain into two separate branches. Since the anisotropy is only 25% of that associated with the c axis, the splittings will be quite small, probably about 0.2×10^{12} cps. The origin of the broad distributions observed from the magnetic excitations below T_N is probably the slightly different frequencies of these modes and of the modes in the different domains. Above T_N it is likely that the broad distributions arise from the paramagnetic width of the levels.

5. Temperature Dependence of Magnetic Properties

The Néel temperature of this model of CoO has been computed using molecular-field theory and neglecting the tetragonal distortion. The value obtained, 239 ± 2°K, is in reasonable agreement (18%) with the observed Néel temperature of 293°K. When distortion was allowed for, the transition temperature was essentially unchanged at 240°K. The calculations were performed within the molecular-field approximation by finding the values of the sublattice spin $\langle S\rangle_{\rm av}$ as a function of temperature. The values of $\langle S\rangle_{\rm av}$ were determined self-consistently as described earlier for the value of the distortion c, at each temperature, that minimized the free energy. The Hamiltonian was

$$\lambda'\mathbf{l}\cdot\mathbf{S}+2J_2Z_2\langle S\rangle_{\rm av}S^z+c[l_z{}^2-\tfrac{1}{3}l(l+1)]+Ac^2,$$

where A is related to the elastic constant for distortion along the c axis, and may be determined from the value of the distortion deduced from the low-temperature neutron results as described in Sec. IV 3. The resultant temperature dependences of the distortion and of the sublattice spin $\langle S\rangle_{\rm av}$ are shown in Fig. 8. The distortion decreases with increasing temperature but is finite just below the transition temperature. The distortion has almost no effect on the sublattice spin, as may be seen from the curve of $\langle S\rangle_{\rm av}$ when distortion is neglected, and consequently the transition temperature is insensitive to distortion. This is a consequence of the relative unimportance of the distortion energy compared with the exchange and spin-orbit terms in the Hamiltonian.

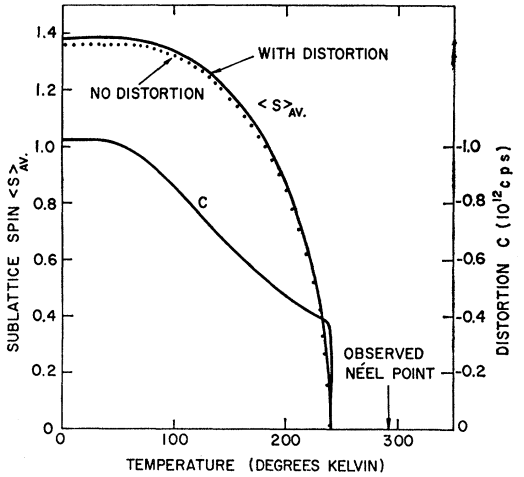

FIG. 8. The temperature dependence of the sublattice spin and distortion as a function of temperature. The molecular-field approximation was used and the distortion computed to minimize the free energy. The sublattice spin neglecting distortion is also shown.

6. Discussion of Results

Our results and theory may be compared with the far-infrared results of Milward.[9] At 4.2°K he observed a peak at a frequency of 4.2×10^{12} cps and two 'broad bands' at 5.0 and 5.7×10^{12} cps. The latter are in agreement with our results, but the former, and his

failure to observe a peak in the region $7–8\times10^{12}$ cps, are not. The low-frequency peak, which was interpreted by Milward as arising from a magnon mode of very small wave vector, became very much weaker and broader as the temperature was raised to 77°K; it might well become submerged in the background noise at 110°K, and thus be consistent with our failure to observe it in the neutron-scattering experiments at that temperature. However, the existence of such a magnon mode is not consistent with the theoretical description developed in Secs. IV 3 and IV 4. Moreover, the unusual behavior with respect to temperature and magnetic field of this low-frequency peak tends to support the possibility, as noted by Milward, that it might be associated with an impurity in his specimen. Infrared-absorption measurements on different CoO specimens would presumably settle this question.

No striking experimental evidence was obtained for a magnon-phonon interaction. The absence of the effect is seen to be reasonable when the mechanism for the coupling of magnons and phonons is considered. These may interact because the electrostatic field of the ions is altered by the presence of a phonon, and this in turn disturbs the energy levels. In the case of UO_2, where a strong interaction was observed,[19] the anisotropy from the crystal field in the ground state is comparable with the molecular-field energy. In CoO, however, this is not the case, as the distortion energy is only about 15% of the molecular-field energy. Since the magnon-phonon interaction in UO_2 is about 20% of the anisotropy energy, we expect a magnon-phonon interaction in CoO of about 0.15×10^{12} cps. This is well below the experimental resolution, and although not negligible, would not be expected to influence the experimental results of Sec. II significantly.

V. CONCLUSIONS

We have observed the low-lying excitations in CoO by using the technique of slow neutron scattering. The results are believed to be largely complete up to a frequency of about 10×10^{12} cps for excitations propagating along the main symmetry directions at 110°K and above the Néel temperature. Many of these excitations are typical of the phonon-dispersion relation for a material with the rock-salt structure, and have been used to obtain the parameters of a shell model for the lattice dynamics of CoO.

The other two branches are believed to arise from electronic transitions. In the paramagnetic phase the results may be explained quite satisfactorily if the spin-orbit coupling parameter is 40% that of the free ion. In the antiferromagnetic phase the results are in at least qualitative agreement with a model with an almost negligible nearest-neighbor exchange constant of 0.021 a second nearest-neighbor constant of 0.347, and a tetragonal distortion parameter of −0.7 (all quantities in units of 10^{12} cps). In this calculation only the two lowest excited states were included. Agreement might well be improved by including more states as the interaction with the higher states would tend to reduce the dispersion of the upper state.

The model also neglected the interaction with the next atomic $4p$ state (Fig. 6) and also the effect of the spin-orbit interaction in coupling the ground Γ_4 state to the Γ_5. Kanamori[10] includes both these effects, but it was considered that the present experimental data did not warrant the inclusion of these comparatively small perturbations. Undoubtedly, the most striking feature of the model is the value of the spin-orbit coupling parameter. It is very difficult to understand how the covalent bonding of the Co^{2+} to its neighboring oxygen ions or the interaction with the higher states can reduce it so much. The reduction of the effective spin-orbit parameter may constitute evidence for a dynamic Jahn-Teller effect as described by Ham.[23]

A more complete understanding will only result when more detailed experiments have been done. Experiments at much greater resolution might well separate the different branches present in the broad bands of excitations seen at present. In this connection, a single-domain specimen might be useful. Measurement of the excitations at higher frequencies would permit a more detailed check of the theory. The temperature dependence of the magnetic excitations also appears to be of interest, especially at low temperatures, for comparison with Milward's infrared result and near the Néel temperature where the frequencies of the magnetic levels should be changing rapidly with temperature. It is planned to attempt some of these experiments in the future.

ACKNOWLEDGMENTS

Invaluable technical assistance throughout this work was provided by E. A. Glaser, M. McManus, and D. A. Betts.

[23] F. S. Ham, Phys. Rev. **138**, A1727 (1965).